JACS JOURNAL OF THE AMERICAN CHEMICAL SOCIETY

Article

Cite This: J. Am. Chem. Soc. 2019, 141, 12804−12814

pubs.acs.org/JACS

Assembling a Natural Small Molecule into a Supramolecular Network with High Structural Order and Dynamic Functions

Qi Zhang,[†,∥] Yuan-Xin Deng,[†,∥] Hong-Xi Luo,[‡] Chen-Yu Shi,[†] Geoffrey M. Geise,[‡] Ben L. Feringa,[*,†,§] He Tian,[†] and Da-Hui Qu[*,†]

[†]Key Laboratory for Advanced Materials and Joint International Research Laboratory of Precision Chemistry and Molecular Engineering, Feringa Nobel Prize Scientist Joint Research Center, School of Chemistry and Molecular Engineering, East China University of Science and Technology, 130 Meilong Road, Shanghai 200237, China

[‡]Department of Chemical Engineering, University of Virginia, 102 Engineers' Way, P.O. Box 400741, Charlottesville, Virginia 22904, United States

[§]Centre for Systems Chemistry, Stratingh Institute for Chemistry and Zernike Institute for Advanced Materials, Faculty of Mathematics and Natural Sciences, University of Groningen, Nijenborgh 4, 9747 AG Groningen, The Netherlands

Supporting Information

ABSTRACT: Programming the hierarchical self-assembly of small molecules has been a fundamental topic of great significance in biological systems and artificial supramolecular systems. Precise and highly programmed self-assembly can produce supramolecular architectures with distinct structural features. However, it still remains a challenge how to precisely control the self-assembly pathway in a desirable way by introducing abundant structural information into a limited molecular backbone. Here we disclose a strategy that directs the hierarchical self-assembly of sodium thioctate, a small molecule of biological origin, into a highly ordered supramolecular layered network. By combining the unique dynamic covalent ring-opening-polymerization of sodium thioctate and an evaporation-induced interfacial confinement effect, we precisely direct the dynamic supramolecular self-assembly of this simple small molecule in a scheduled hierarchical pathway, resulting in a layered structure with long-range order at both macroscopic and molecular scales, which is revealed by small-angle and wide-angle X-ray scattering technologies. The resulting supramolecular layers are found to be able to bind water molecules as structural water, which works as an interlayer lubricant to modulate the material properties, such as mechanical performance, self-healing capability, and actuating function. Analogous to many reversibly self-assembled biological systems, the highly dynamic polymeric network can be degraded into monomers and reformed by a water-mediated route, exhibiting full recyclability in a facile, mild, and environmentally friendly way. This approach for assembling commercial small molecules into structurally complex materials paves the way for low-cost functional supramolecular materials based on synthetically simple procedures.

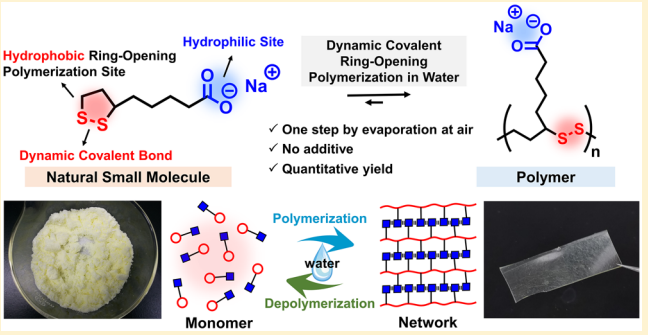

INTRODUCTION

Molecular self-assembly has emerged as a topic of great significance in general as it holds great promise toward next generations' functional materials.[1−5] A variety of approaches followed by chemists triggered the rapid expansion of supramolecular self-assembly as an interdisciplinary area.[6,7] Using a "bottom-up" strategy, complex materials can be prepared by highly programmed self-assembly of small-molecule building blocks,[8−12] which might enable the precise tailoring and manipulation of matter and functional control along various length scales.[13,14] Until recently, supramolecular self-assembly in artificial molecular systems had exhibited a predominant capability to form morphology-controlled multidimensional structures, such as amphiphilic vesicles/micelles,[15] gels,[16,17] linear polymers,[18] and the cross-linked networks.[19] The hierarchical self-assembly of these primary structures can further result in truly unique soft matter.[20−22] The diversity, complexity, and functionality of these materials can be especially striking if the molecular self-assembly of the small building blocks is precisely controlled in a programmed mode,[23−25] also signifying the opportunity to program information via the molecular self-assembly mode into molecular structures as information.[26] In this context, structural information in a precursor molecule would enable the precisely controlled self-assembly of small molecules into large-scale assemblies with desirable organized structures and properties. However, to meet the rising need for advanced

Received: May 29, 2019
Published: July 26, 2019

DOI: 10.1021/jacs.9b05740
J. Am. Chem. Soc. 2019, 141, 12804−12814

materials with sophisticated and even multiple functions, tedious synthetic routes are frequently required to prepare precursor molecules via complex chemical modifications, whereas simple buildings blocks leading to complexity would be highly desirable.

Very recently, we explored a small molecule of biological origin, called as thioctic acid, which is a naturally tailored building block that readily forms an amorphous supramolecular network, taking advantage of its disulfide-containing main chain cross-linked by hydrogen bonds and metal-carboxyl complexes,[27] which can be easily prepared by a solvent-free mild method. Although such an amorphous network exhibits potential applications in flexible and wearable materials,[28−32] the disordered cross-linking of the polymer chains hardly produces structurally ordered polymeric materials, which play a crucial role in many other areas, such as liquid crystals,[33−35] soft actuators,[36−40] ionic transport membranes,[41] and high-strength materials.[10,42] Herein, we focus on how this naturally tailored small molecule can be programmed by strategic molecular engineering to realize its precise self-assembly into long-range-order supramolecular architectures. We hope that exploring such a dynamic supramolecular self-assembly process toward structurally ordered assemblies could provide a new generation of molecular tools for the design and construction of supramolecular systems as well as natural product-based polymer materials.[43]

On the basis of this hypothesis, we demonstrate a rational derivation on the natural structure of thioctic acid by simple deprotonation to form amphiphilic sodium thioctate (ST). This simple small molecule can self-assemble into primary linear polymers at high concentrations by dynamic covalent ring-opening-polymerization (ROP), which undergo further self-organization into a highly ordered supramolecular network with a large-scale layered structure using a facile evaporation process. This is to the best of our knowledge an unprecedented example of directly assembling simple small molecules into supramolecular materials with high structural order, which is attributed to the naturally programmed structural information in this unique small-molecule building block. The dynamic covalent polymeric backbones and structural-water-cross-linked layered network simultaneously render the polymeric materials with good mechanical properties, humidity-actuated ability, and closed-loop recyclability.

RESULTS AND DISCUSSION

Design Concept and Aqueous Self-Assembly. Structurally ordered assemblies are generally created by highly synergetic intermolecular interactions. The coexisting multiple species involved in molecular self-organization should be highly hierarchical in binding affinity as well as spatial distribution.[44] The thermal one-pot solvent-free polymerization of thioctic acid was a fast and homogeneous assembly process resulting in amorphous assemblies.[27] Structurally ordered self-assembly mostly involves a slow and thermodynamically controlled process, with relatively low growth rate kinetics to push the dynamic equilibrium toward a thermodynamically stable state.[22] Therefore, two issues should be addressed to realize the ordered self-assembly of thioctic acid: (i) the self-assembly process should not be instantaneous but be programmed with longer time scales, and (ii) multiple molecular interactions with different binding affinities should be introduced to enable a hierarchical self-assembly process with distinct spatial distribution. Notably, the order (or sequence in time) of these hierarchical molecular recognition processes should be also programmed in a precise and desirable pathway.

On the basis of these preconditions, we notice the unique structural features of thioctic acid for potential amphiphilic molecules. The terminal carboxylic group can be deprotonated to form a hydrophilic carboxylate group, while the five-membered disulfide-containing ring is hydrophobic, and the middle C_4-methylene chain links the hydrophilic and hydrophobic parts as a typical amphiphilic structure (Figure 1A).

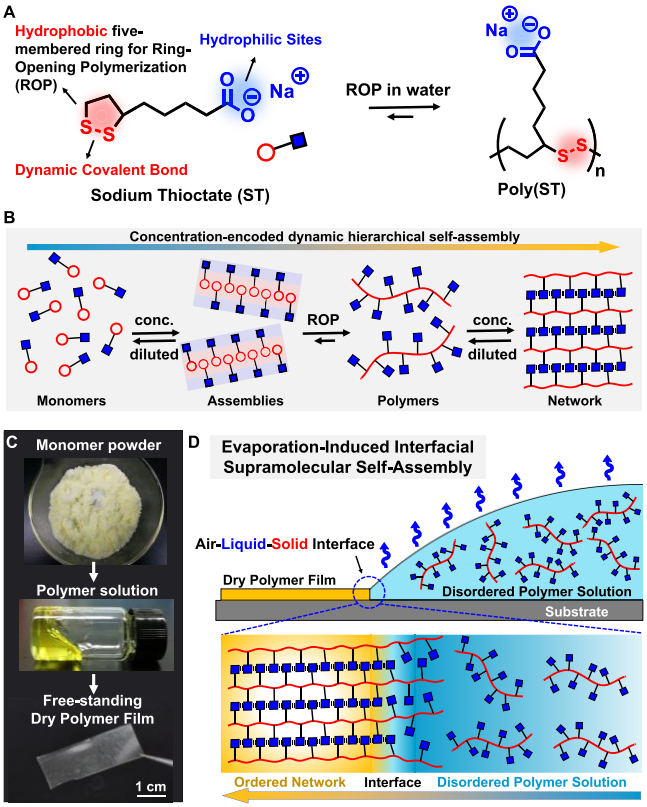

Figure 1. Self-assembly process of sodium thioctate in water. (A and B) Molecular structures (A) and schematic representation (B) of the ST monomers, ST polymers, and their networks. (C) Photographs of the ST crystalline powder, viscous ST polymer solution, and the resulting free-standing flexible solid film. (D) Schematic mechanism of the evaporation-induced interfacial supramolecular self-assembly from disordered polymers in aqueous solution to dry-ordered film network.

This amphiphilic feature could work as structural information for molecular recognition, driving the self-organization of these small-molecule building blocks toward a more thermodynamically stable situation, in which the hydrophobic five-membered rings tend to aggregate to decrease interaction with the surrounding high-energy water molecules. This primary amphiphilic self-assembly further triggers the secondary dynamic covalent ROP reaction by the intermolecular dynamic covalent exchange of disulfide bonds facilitated by the increased intermolecular proximity. Furthermore, the subsequent self-assembly can be enabled using the outer hydrophilic carboxylate groups which recognized each other to form ionic bonds after the removal of solvent, forming an ionic-bond-cross-linked polymeric network (Figure 1B). As a consequence, these features enable the complex hierarchical self-

DOI: 10.1021/jacs.9b05740
J. Am. Chem. Soc. 2019, 141, 12804−12814

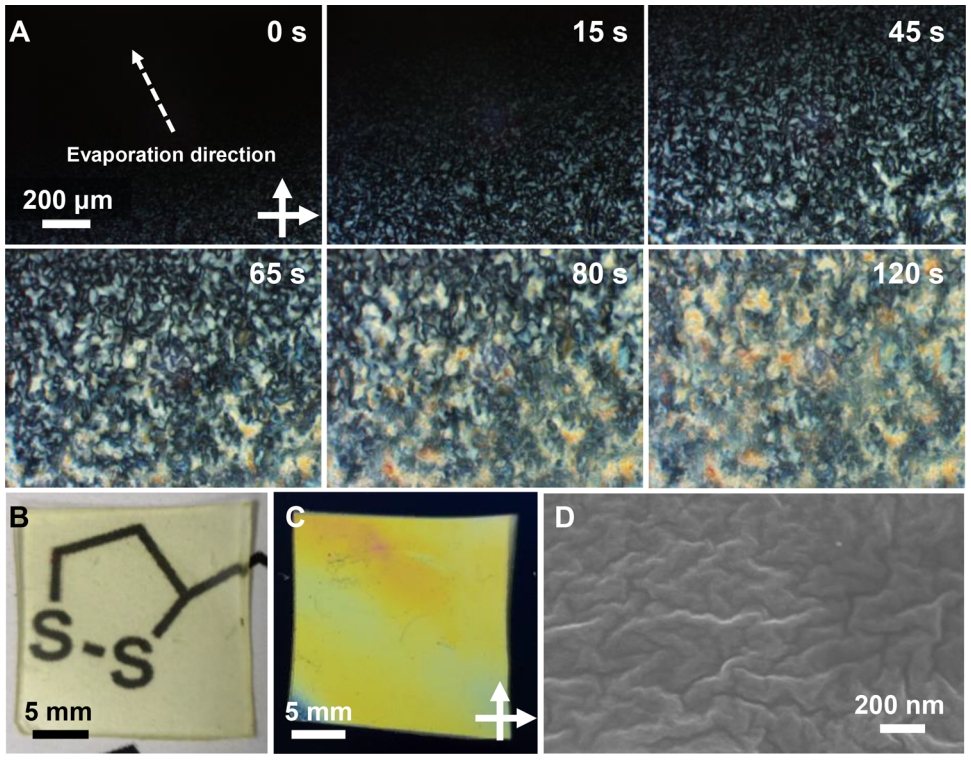

Figure 2. (A) Real-time detection of the formation of a crystalline-phase structure, upon water evaporation, by polarized optical microscopy. The colored bright spots indicated the presence of ordered crystallites in the corresponding region. (B) Photographs of a poly(ST) polymer film with natural light showing good transparency. (C) Photographs of a poly(ST) polymer film under polarized light suggesting the extensive presence of ordered crystalline regions. (D) SEM images of poly(ST) polymer film.

assembly from small molecules to form three-dimensional polymeric networks.

Gram-scale ST monomers can easily be obtained by the quantitative deprotonation reaction of thioctic acid with sodium hydroxide in ethanol and subsequent filtration, yielding a light-yellow crystalline powder with high water-solubility (over 400 g/L at 298 K). Dissolving ST powder in water resulted in a homogeneous yellow solution, and the concentrated solution (over 200 g/L) exhibited remarkably increased viscosity (Figure 1C), suggesting polymerization. The formation of ring-opened linear poly(ST) polymer was confirmed by distinctive proton shifts[27] and broadening in the ^{1}H NMR spectrum (Figure S1). Meanwhile, the disulfide-containing five-membered ring can be considered a chromophore because of its characteristic absorption maximum at 330 nm (Figure S2A), which originates from the red-shifted absorption of the disulfide group as a result of five-membered-ring tension.[45] Therefore, the absorbance of this chromophore can be used to detect the dynamic covalent ROP process in aqueous solution.[46] At concentrations lower than 150 g/L, the absorbance versus concentration plot of ST strictly follows Lambert–Beer's law, while the absorbance of the 200 g/L sample exhibited a remarkable decrease in slope (Figure S2B), confirming the ROP process. It should be noted that the polymers and monomers coexisted in a concentrated state due to the presence of absorption at 330 nm. The coexistence is attributed to the dynamic nature of the dynamic covalent self-assembly process.[47] The viscous polymer solution exhibited excellent stability at room temperature, without phase separation or viscosity decrease after three months of observation (Figure S3). At an extremely high concentration (400 g/L), the high viscosity can even support the formation of a transparent hydrogel network at relatively low temperature (10 °C) (Figure S4), which can be rationalized on the basis of the formation of high-molecular-weight polymers and ionic-bond cross-links. The hydrogel is labile to concentration decrease and temperature increase, which would transform the material into a viscous polymer solution upon heating or dilution by water, revealing the dynamic reversible nature of this supramolecular polymer.

Evaporation-Induced Interfacial Self-Assembly. As demonstrated previously, the key to forming a structurally ordered network includes a long-time growth process and temporal distribution of the hierarchical self-assembly steps programmed in a precise and desirable pathway. The equilibrium states of the hierarchical dynamic self-assembly processes of poly(ST) are strongly dependent on concentration, indicating that a concentration increase can be a key factor to drive the proposed dynamic self-assembly equilibrium. On the basis of this notion, we employ a solvent-evaporation strategy to direct the hierarchical self-assembly process in a thermodynamically controlled manner. The evaporation-directed method has been used in controlling uniform assembled morphology of nanostructures.[48] Here we demonstrate that the evaporation process enables a dynamic covalent ROP templated by interfacial self-assembly (Figure 1D), i.e., the edge of the ellipsoidal droplet bears the fastest evaporation kinetic, thus undergoing nucleation at the edge region when the localized solution is oversaturated. Upon further solvent evaporation, the air/liquid/solid interface moves slowly along the evaporation direction, where the linear polymers assemble and grow at the three-phase interface, eventually producing a structurally ordered layered network. We propose that the interfacial confinement effect could well

DOI: 10.1021/jacs.9b05740
J. Am. Chem. Soc. 2019, 141, 12804–12814

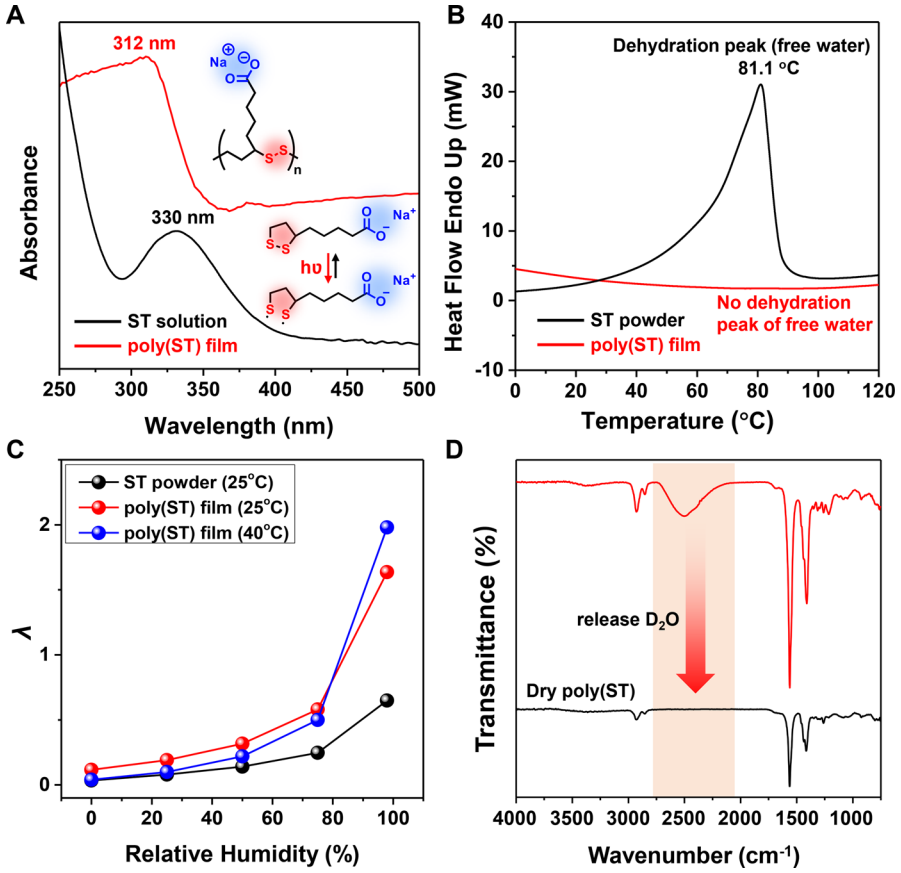

Figure 3. (A) UV−vis absorption spectra of ST aqueous solution (1 g/L) and dry poly(ST) film. (B) DSC curves of the ST powder and poly(ST) polymer film. (C) Hydration number (λ) measurements under varying relative humidity. (D) FT-IR spectra of the poly(ST) polymer film before (red line) and after (black line) release of adsorbed D_2O.

organize these unique small-molecule building blocks by producing a localized concentration gradient at the interface. Therefore, this whole process from small molecules (ST) to polymeric network poly(ST) can be identified as an evaporation-induced interfacial self-assembly (EIISA) route.

The EIISA process can be performed readily by dispensing the ST aqueous solution on a glass or polyethylene substrate followed by slow evaporation at ambient conditions, resulting in a free-standing dry solid polymeric film, which can be easily separated from the substrate (Figures 1C and S5 and S6). Polarized optical microscopy was employed to detect the self-assembly process with evaporation-induced interface movement in real time (Figures 2a and S7). Initially, the aqueous solution of ST is homogeneous and isotropic, hence exhibiting an invisible birefringence property. With the evaporation of the solution, a bright pattern of cyan color appeared to form an interface, suggesting the formation of structurally ordered assemblies. Then the interface moved along the evaporation direction, leaving the progressing route with expanded cyan patterns. The bright cyan regions changed into yellow patterns with further evaporation, which can be attributed to the shrinking of the assembled layers induced by water release.

The resulting polymer film exhibited good optical transparency (Figure 2B) and showed a remarkable birefringence feature (Figure 2C), indicating long-range-ordered self-assembly in bulk phase. The identical peak signals from the ST monomer powder and polymer film in the Fourier-transform infrared (FT-IR) spectrum (Figure S8) and Raman spectra (Figure S9) indicated similar chemical structures both before and after the EIISA process, confirming the absence of other side reactions. Scanning electron microscope (SEM) images (Figures 2D and S10) showed the compact surface morphology of the resulting films. Wrinkled nanostructures were observed, which might be the result of surface folding induced by solvent evaporation.

Structural Characterization of the Resulting Polymers. The polymeric nature of the resulting poly(ST) film can be confirmed by its optical properties. The diluted aqueous solution of monomer ST (1 g/L) containing a five-membered ring exhibited a characteristic absorption at 330 nm (Figure 3A) and photochemical excitation induced the ring-opening process to produce disulfide radicals, which were rebonded intramolecularly due to the uninitiated primary amphiphilic self-assembly at 1 g/L. The UV−vis reflection spectrum of the resulting poly(ST) film showed a peak at 312 nm, while no distinctive absorption was visible at 330 nm, indicating the absence of ST monomers. Differential scanning calorimetry (DSC) on the ST powder also showed a distinctive dehydration peak at 81.1 °C (Figure 3B), and no dehydration peak was observed at this region in the poly(ST) film, indicating a higher binding energy of bound water in the poly(ST) film compared to the powder. This result also suggests complete polymerization in the poly(ST)film because of the lack of a dehydration peak in the ST monomer thermogram.

The water-sensitive ionic bonds in the network create the poly(ST) film's humidity-responsive capability. The dry robust polymer film can adsorb water molecules from the air, leading

DOI: 10.1021/jacs.9b05740
J. Am. Chem. Soc. 2019, 141, 12804−12814

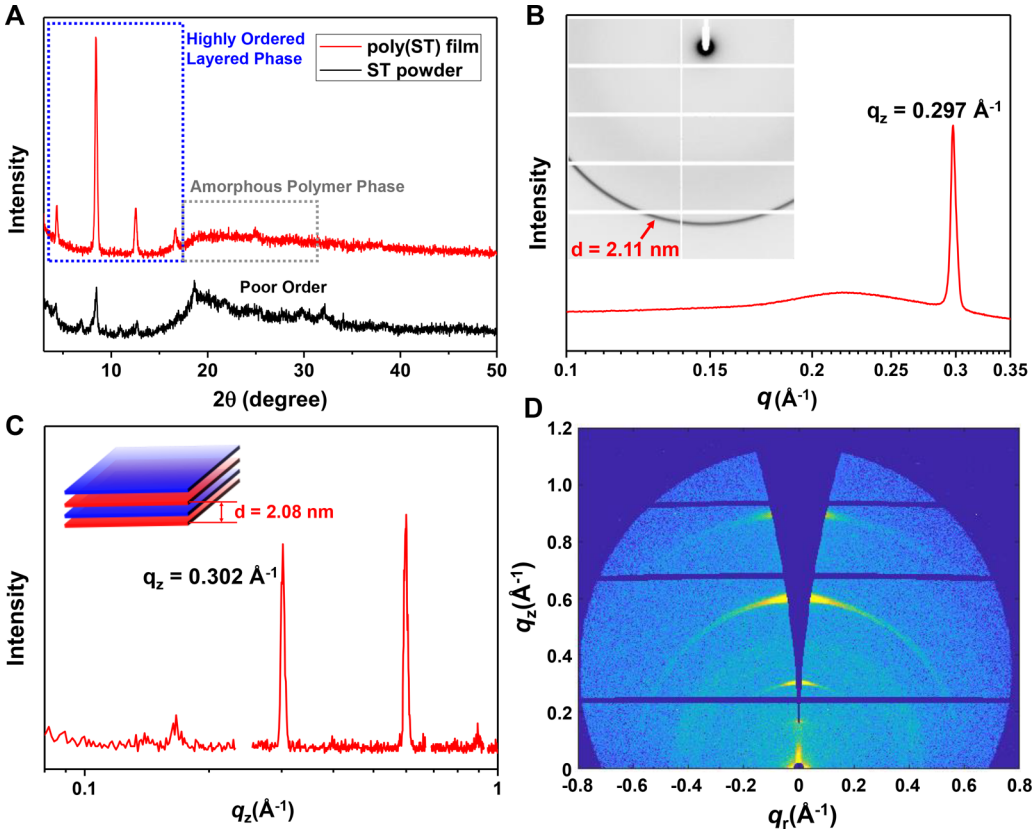

Figure 4. (A) XRD patterns of the ST monomer powders and the resulting poly(ST) film. (B) Synchrotron radiation SAXS pattern of the poly(ST) film. Inset image shows the distinctive scattering ring of the sample. (C) One-dimensional GIWAXS plot of the poly(ST) film. Scattering intensity is plotted versus q_z. (D) Two-dimensional GIWAXS pattern of the poly(ST) film.

to an increase in hydration that scales with the relative humidity (RH) of the air (Figure 3C). To quantitatively evaluate the hydration number (λ, defined as the number of water molecules per carboxylate group) of the humidity-responsive poly(ST) film, humidity-varying thermogravimetry was performed on the ST powder and poly(ST) film (Figure S11–S13). The ST powder exhibited a low λ value from 0.03 (RH = 0%) to 0.65 (RH = 98%) at 25 °C. However, the poly(ST) film bear a much higher λ which increased from 0.12 (RH = 0%) to 1.64 (RH = 98%) at 25 °C, and an increased temperature (40 °C) led to a slight difference of this range from 0.04 (RH = 0%) to 1.98 (RH = 98%). The higher λ number of poly(ST) film is attributed to its ordered layered structure, wherein the hydrophilic carboxylate groups associate to form interlayer water channels by ionic bonding. This enables the abundant spatial sites and carboxylate interlayers as the water diffusion channels. However, for the ST powder samples, the poor structural order resulted in the limited diffusion and hydration in the inner cores. On the contrary, notably slower hydration kinetics of poly(ST) film were observed compared with that of ST powder (Figure S14), which is attributed to the ordered layered structure of periodically alternating hydrophobic/hydrophilic layers. The sandwich-like layers confined the hydrophilic water channels in two-dimension between the hydrophobic polymer mainchain phase, thus slowing the hydration kinetics in the low humidity regions (Figure S15). The observed differences in hydration thermodynamics and kinetics between the ST powders and poly(ST) films further supports the proposed long-range-order layered structure with water channels in the poly(ST) films formed by EIISA method.

The water adsorption mechanism was confirmed by analysis of the FT-IR spectra (Figure S16). A slight IR shift for the carboxylate groups was observed from 1562 to 1552 cm^{-1} after adsorbing water, which was attributed to the hydration of the carboxylate groups. The disappearance of a shoulder peak at 1432 cm^{-1} after water adsorption also suggested the hydration of the carboxylate groups while the increased peak around 3400 cm^{-1} indicated bound water in the network. The release process was further confirmed by D_2O because of its characteristic feature signal at around 2500 cm^{-1} (Figure 3D). The D_2O molecules adsorbed in the poly(ST) network were found to be totally released by placing the film into dry air condition at room temperature, indicating that the bound water in the network can be fully exchanged in an ambient atmosphere.

X-ray diffraction and scattering tests (Figure 4) were performed to characterize the structural order of the resulting poly(ST) film. X-ray diffraction (XRD) of the dry poly(ST) film showed sharp and high-intensity diffraction peaks in the small angle regime (less than 20°), indicating a typical, highly ordered structure at the nanoscale (Figure 4A). The peak at 4.38° was attributed to a layer distance of 2.02 nm (calculated by the Bragg equation). The periodic signals also suggested a highly ordered layered structure. Meanwhile, the broad and low peak at around 23° suggested an amorphous hydrophobic disulfide-containing polymer main chain phase.[27] As a reference, ST powder was also measured, which showed a largely amorphous structure with poor structural order,

DOI: 10.1021/jacs.9b05740
J. Am. Chem. Soc. 2019, 141, 12804−12814

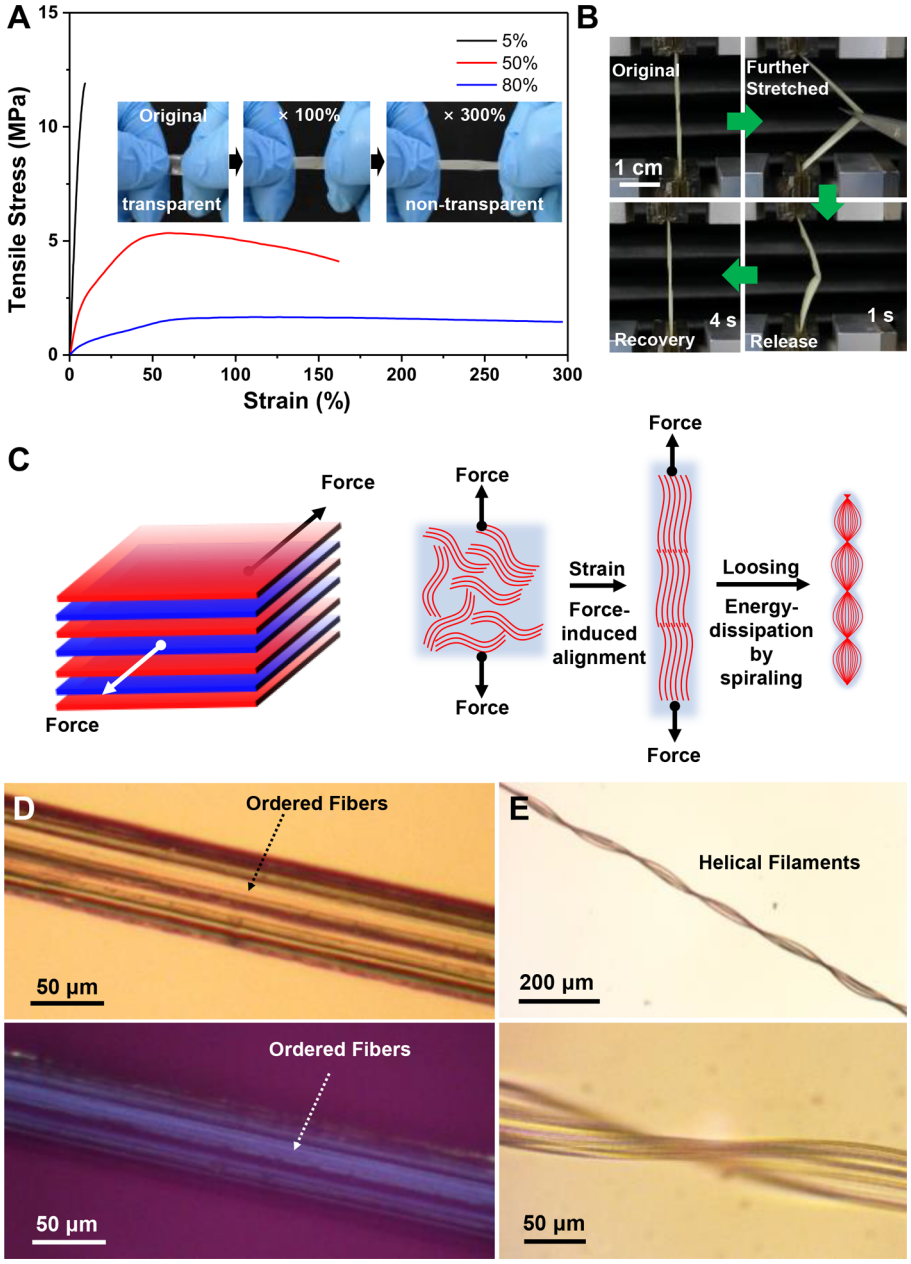

Figure 5. (A) Tensile stress curves of the poly(ST) film under different RH (5%, 50%, and 80%, respectively). Inset photographs show the stretched poly(ST) film (RH = 80%). (B) Photographs show the rapid relaxation behavior of a stretched poly(ST) film (RH = 80%). (C) Schematic representation of the tension-induced alignment of the elastic poly(ST) film. (D) Optical microscope images of the polymer filaments made by stretching the hydrated poly(ST) films (RH = 80%). Bright field (top) and polarized light field (bottom) show the ordered fibers paralleled with the tension direction. (E) Schematic representation and optical images of the helical filaments which are formed by mechanical tension followed by relaxation.

indicating the significance of the EIISA method for the formation of structurally ordered poly(ST) film. Small-angle X-ray scattering (SAXS) showed a sharp scattering signal at 0.297 $Å^{-1}$ (Figure 4B), indicating the high structural order with 2.11 nm spacing grazing-incidence wide-angle X-ray scattering (GIWAXS) further revealing the highly ordered layered structure of the resulting poly(ST) film (Figure 4C,D). The periodic one-dimensional scattering sharp peaks and two-dimensional high-intensity scattering rings confirmed the highly ordered layered structure in the poly(ST) network.[41] The observed scattering vector q = 0.302 $Å^{-1}$ can be attributed to the layer distance of 2.08 nm of the resulting poly(ST) film, which was consistent with the XRD and SAXS results, confirming the interlayer distance as 2.1 nm of the layered poly(ST) film.

Rheology and Mechanical Properties. The storage moduli (G') was higher than the loss moduli (G'') over the entire range of frequencies (Figure S17A) and also exhibited a single plateau region in the dynamic moduli. It should be noted that the moduli can be commensurate with that of the previously reported covalent-/iron(III)-*co*-cross-linked network,[27] even in the absence of a covalent cross-linker or iron(III) ions in the poly(ST) film. In a temperature-varied experiment (Figure S17B), moduli and viscosity slightly decreased with rising temperatures, which might be attributed to the thermo-labile disulfide bonds in the polymer main chain.

DOI: 10.1021/jacs.9b05740
J. Am. Chem. Soc. 2019, 141, 12804−12814

The dry polymer film exhibited robust mechanical properties with a Young's tensile modulus of 168.8 MPa (Figure 5A), which was attributed to the ordered layered structure and high-affinity ionic bonds in the dry network. Interestingly, an increased hydrated degree led to a remarkable decrease in the tensile strength but also an increasing flexibility and stretchability (Figure 5A). This observation was attributed to the hydration of high-affinity ionic groups by bound water molecules, which worked as a lubricant-like structural water[49−51] by forming weak but dynamic hydrogen bonds in the interlayers of the network. The hydrated poly(ST) film exhibited a fast relaxation-recovery ability (Figure 5B and Movie S1) and an elasticity in a cyclic experiment (Figure S18). In the highly hydrated state (RH > 95%), the hydrated poly(ST) polymer turned very soft and viscous, showing a lower birefraction degree (Figure S19) and amorphous diffraction peaks (Figure S20), which is attributed to the formation of the hydrogen-bond-cross-linked network.

A notable decrease in optical transparency was observed upon stretching the elastic poly(ST) film (Figure 5A inset), which is the result of tension-induced order of the stretched polymer chain (Figure 5C). The alignment of microfibers along the tension direction can be observed in brightfield and polarized- light-field by optical microscopy (Figure 5D). Interestingly, an instant loosening of the stretched filaments resulted in a rapid formation of helical filaments, in which the aligned order was maintained. This transformation might be the result of an energy dissipation pathway originating from imposed potential energy within the stretched filaments. The helical structure was stable in dry conditions (RH < 50%) for several weeks, while they lost their shape and inner order upon exposure to highly humid conditions due to the decreased structural order by adsorbed water. Hence, the structural order of the layered network is necessary for this relaxation-induced spiraling behavior.

Applications as Dynamic Materials. The resulting structurally ordered layered supramolecular film simultaneously integrates dynamic covalent mainchains and supramolecular interaction in a single network, including noncovalent ionic bonds, hydrogen bonds of bound water, the van der Waals interaction of folded and packed polymer chains, and dynamic covalent disulfide bonds. These distinct features result from the dynamic nature of the polymer main chains with a high-proportion of disulfide groups, which might give this material unique dynamic properties and applications. The self-healing ability of the resulting poly(ST) films was confirmed by scratching experiments (Figure S21A). The film samples with varied degrees of hydration exhibited different self-healing capability, which was activated at the RH regions over 50%, while the dry samples showed no self-healing. In a typical healing experiment, a scratch can be healed almost completely in 12 h. Considering the switchable mechanical properties depending on reversible water adsorption/release, a water-mediated self-healing capability of mechanically robust materials is realized. Self-healing robust materials are very rare because of the limited interface mobility.[52] In our case, the damaged dry robust poly(ST) film can be "lubricated" by adsorbing water to enhance the interface mobility and dynamic properties. Then the damage can be healed, taking advantage of the reversible polymeric main chains and dynamic supramolecular interactions (Figure S21B), followed by releasing the water molecule upon drying to afford repaired and robust films.

Considering the three-dimensional multilayer polymer film, the humidity-induced expansion motion can be expected to be used as a humidity-induced actuator based on the supramolecular network. Placing a flat poly(ST) polymer film above a moisture generator would generate an asymmetric humidity gradient environment, with the film region near the water adsorbing more water molecules than the region away from the water, thus producing an asymmetric volume expansion degree (Figure 6A,B). In a typical experiment, a polymer film can

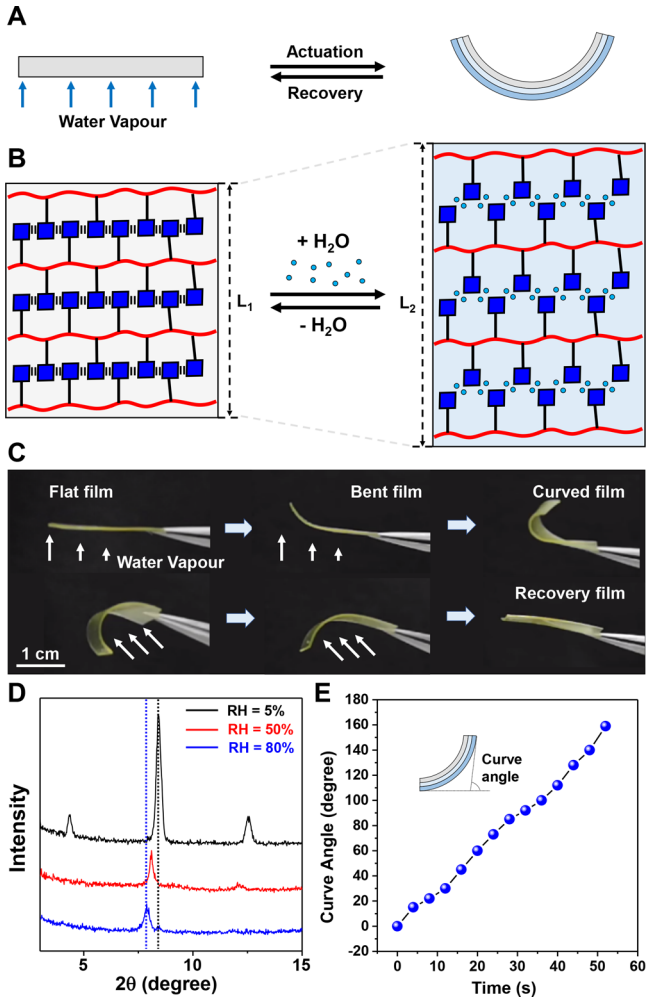

Figure 6. (A) Schematic representation of the humidity-induced actuation behavior of poly(ST) polymer film. The blue arrows mean the humidity gradient direction. (B) Schematic representation of the expansion mechanism of the interlayers. (C) Photographs show the capability of poly(ST) polymer film acting as a humidity-responsive actuator. (D) XRD patterns of the poly(ST) film under varied RH. (E) Actuating kinetic curve of the bending polymer film to water vapor.

transform from a flat shape into a bent one, while the inverse process can be driven by drying (Figure S22) or triggering the other less-hydrated side of the film (Figure 6C). The humidity-induced layer expansion can be confirmed by XRD patterns (Figure 6D), in which the diffraction angle of the film decreased with the increased RH, indicating the increase of layer distances after adsorbing water molecules. The kinetic curve showed a linear correlation with time and a responding rate of 2.9 deg/s (Figure 6E). Although several polymer actuators have been reported,[53,54] the actuator presented here

DOI: 10.1021/jacs.9b05740
J. Am. Chem. Soc. 2019, 141, 12804−12814

based on the poly(ST) network, is totally cross-linked by dynamic covalent and supramolecular interactions instead of covalent cross-linkers, with an extremely simple preparation method initiated from natural small molecules.

The realization of recyclability in synthetic polymers is a key topic toward environment and energy issues. Though many polymer materials can be degraded or reprocessed, it has been highly challenging to realize fully recyclable polymers which can be transformed into monomer feedstocks in a mild and facile condition.[55−60] Here we propose a polymer-recycling strategy by dynamic covalent ROP. Interestingly, dissolving the poly(ST) polymer film in water resulted in a monomer/oligomer solution (Figures 7A and S23), which was confirmed

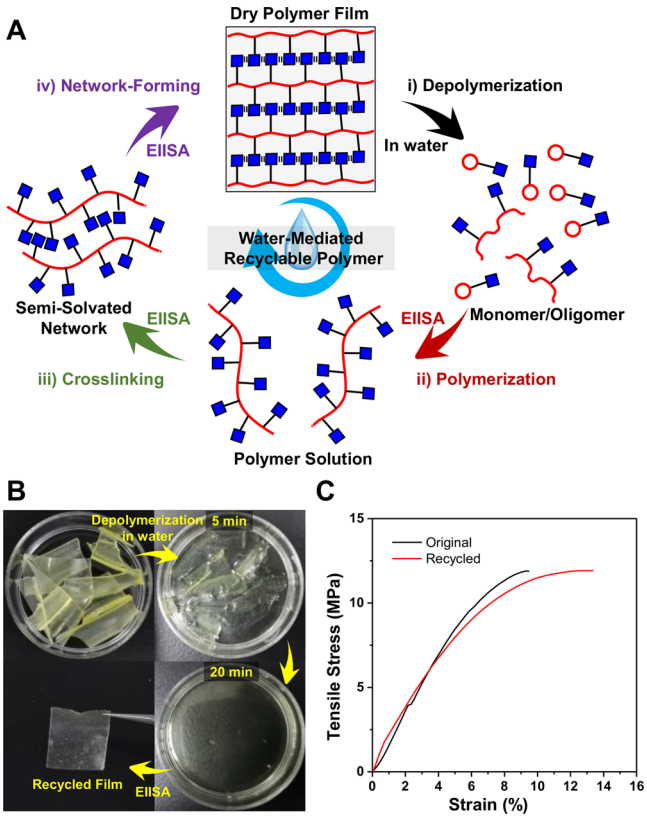

Figure 7. (A) Schematic representation of the water-mediated recycling process of the poly(ST) films. (B) Photographs show the recycling process of the polymer film fragments into a new polymer film. (C) Tensile stress curve of the original and recycled poly(ST) films. The tested samples are dried at room temperature (RH < 10%).

by ^{1}H NMR spectroscopy (Figure S24). This result revealed that the cross-linked polymer network can be efficiently depolymerized into ring-closed ST monomers and oligomers by the addition of excess water. The high degradation efficiency can be also confirmed by the remarkably decreased moduli (below 5 Pa) and viscosity (below 10 Pas) of a degraded aqueous solution (100 g/L) (Figure S25). Then the recycled monomer/oligomers solution can be used to produce recycled polymer film by a similar EIISA process. Therefore, the closed-loop polymer-recycling process simply requires the mediation by water (Figure 7A) while the depolymerization process can be completed in 20 min (Figure 7B). The recycled polymer film exhibited consistent mechanical properties (Figure 7C), indicating the high recycling efficiency of this water-mediated route. Therefore, this polymer exhibits an unprecedented recyclability that bears no organic solvent, no heat, no high pressure, and no special technique, showing a promising potential toward environmentally friendly and energy-saving polymer materials.

CONCLUSIONS

By controlling the dynamic self-assembly of sodium thioctate (ST) in water based on hydrophilic/hydrophobic effects, dynamic covalent ROP, and ionic interactions with evaporation-induced interfacial ordering, we achieved hierarchical self-assembly of a small molecule into a layered supramolecular network with a long-range order. The resulting layered dry network bears alternating layers with hydrophilic ionic stacking and hydrophobic polymer mainchains, with the former being able to bind water molecules to form interlayer water channels. Distinct structural features provide this material with dynamic and adaptive mechanical properties, self-healing capability, and actuation functions. The unique dynamic covalent polymer mainchains can be disassembled into monomers and quantitively reused by a facile room-temperature water-mediated route, providing a conceptually new strategy to design recyclable polymeric materials.

In summary, this supramolecular material based on the self-assembly of deprotonated thioctic acid exhibits simplicity in preparation as well as order and complexity in structure and properties, pushing the versatile supramolecular materials based on thioctic acid from previously disordered elastomers to structurally ordered layers. This work paves the way for what we believe to be one of the fundamental issues in supramolecular chemistry; programming the precisely hierarchical self-assembly of small molecules toward structurally complex architectures, opening new avenues for dynamic polymeric materials in optics, electronics, sensors, coatings, and biomedical systems.

MATERIALS AND METHODS

Materials Preparation. Sodium thioctate (ST) was prepared as bright yellow solid powder by a one-step reaction of equivalent amounts of thioctic acid and NaOH in ethanol/water solution heated under reflux. The ST powder is highly water-soluble and viscous aqueous solution can be obtained with a high concentration up to 300 g/L. In a typical preparation of poly(ST) film, a small volume of poly(ST) solution (300 g/L) was deposited on the substrate by simply drop-coating (the formed area is about 10 cm^2 per 1 mL). The substrate can be glass, plastic dish, or Teflon. Then the polymer solution on the substrate was left in air to allow slow evaporation of the solvent. The evaporation process normally takes 2−6 h depending on the air humidity and the temperature. No remarkable difference was observed in the resulting polymer film obtained in different time within this time regime. The resulting dry polymer can be easily separated from the substrate as a transparent, free-standing, and robust polymer film.

Mechanical Tension Experiments. The stress−strain curves were recorded with an HY-0580 tension machine (HENGYI Company, Shanghai). The tested polymer films were preplaced for at least 2 h at the given RH to reach the adsorption/desorption equilibrium with water. Then the film was quickly fixed onto the tension machine and tested. The whole tension process was completed in 10 min. Considering the low water adsorption/desorption kinetic of the poly(ST) films, the hydration number of the polymer film in mechanical tension experiments can be considered as almost constant. The RH of the testing environment was fluctuated in a limited region (40% ∼ 60%). The film was shaped as a rectangle sample (20 × 10 × 0.5 mm). The initial length was 10 mm. Unless

DOI: 10.1021/jacs.9b05740
J. Am. Chem. Soc. 2019, 141, 12804−12814

otherwise noted, the tensile stress was measured at a constant speed of 10 mm/min. The data were recorded in real time.

Hydration Number Measurement. The hydration thermodynamics and kinetics of poly(ST) film were measurement by a Relative Humidity Thermogravimetric Analyzer (RH-TGA, TA-Q5000 SA). In a typical experiment, a small piece of dry poly(ST) film (~7 mg) was loaded into a metal-coated quartz pan, and the pan was transferred into the humidity chamber of the analyzer. The total gas flow rate (water vapor and N_2) was chosen as 20 mL/min, and different relative humidity values, namely 0%, 25%, 50%, 75%, and 98%, were achieved by changing the relative flow rates of water vapor saturated N_2 and dry N_2 gas. The film was first dried at 60 °C at 0% RH for 4 h (8 h for powder) to remove residual moisture, and the film weight was recorded as the dry weight (W_D). After the initial drying step, the chamber temperature was reduced to a designated value (i.e., 25 or 40 °C) and the RH value was increased stepwise to 98% (hydration) and then reduced stepwise to 0% (dehydration). The film was allowed to equilibrate at each RH value for 12 h (4 h for powder), and the film weight was recorded at the end of each 12 h equilibration step. The hydrated film weight (W_H) at each RH value was taken as the average of the weight recorded during hydration and dehydration ramps. The film hydration number λ [eq(H_2O)/eq(−COOH)] was defined as

$$\lambda = \frac{(W_H - W_D)/MW(H_2O)}{W_D/EW_{ST}}$$

where the EW_{ST} is the equivalent weight of ST and is taken as 228 g/mol.

■ ASSOCIATED CONTENT

Supporting Information

The Supporting Information is available free of charge on the ACS Publications website at DOI: 10.1021/jacs.9b05740.

Additional materials and methods, NMR analysis, additional spectrum characterization, humidity-varied thermogravimetry, rheology experiments, and additional sample photographs (PDF)

Hydrated poly(ST) film exhibiting a fast relaxation-recovery ability (MP4)

■ AUTHOR INFORMATION

Corresponding Authors

*b.l.feringa@rug.nl

*dahui_qu@ecust.edu.cn

ORCID

Hong-Xi Luo: 0000-0003-4824-9385

Geoffrey M. Geise: 0000-0002-5439-272X

Ben L. Feringa: 0000-0003-0588-8435

He Tian: 0000-0003-3547-7485

Da-Hui Qu: 0000-0002-2039-3564

Author Contributions

‖Q.Z. and Y.-X.D. contributed equally to this work.

Notes

The authors declare no competing financial interest.

■ ACKNOWLEDGMENTS

This work was supported by National Natural Science Foundation of China (Grants 21788102, 21790361, 21871084, 21672060, and 21421004), Shanghai Municipal Science and Technology Major Project (Grant 2018SHZDZX03), the Fundamental Research Funds for the Central Universities, the Programme of Introducing Talents of Discipline to Universities (Grant B16017), Program of Shanghai Academic/Technology Research Leader (19XD1421100), and the Shanghai Science and Technology Committee (Grant 17520750100). Geoffrey M. Geise appreciates the support of National Science Foundation under Grant CBET-1752048. Ben L. Feringa acknowledges financial support of The Netherlands Ministry of Education, Culture, and Science (Gravitation program 024.601035). We appreciate Dr. Na Li (BL19U2 beamline of Shanghai Synchrotron Radiation Facility) for her kind help in synchrotron SAXS test and Miss Qi Wei and Prof. Zhijun Ning (ShanghaiTech University) for their kind help in GIWAXS experiments. We thank the Research Center of Analysis and Test of East China University of Science and Technology for help on the material characterization.

■ REFERENCES

(1) Lutz, J. F.; Lehn, J. M.; Meijer, E. W.; Matyjaszewski, K. From precision polymers to complex materials and systems. *Nat. Rev. Mater.* **2016**, *1*, 16024.

(2) Kang, J.; Miyajima, D.; Mori, T.; Inoue, Y.; Itoh, Y.; Aida, T. A rational strategy for the realization of chain-growth supramolecular polymerization. *Science* **2015**, *347*, 646−651.

(3) Freeman, R.; Han, M.; Álvarez, Z.; Lewis, J. A.; Wester, J. R.; Stephanopoulos, N.; McClendon, M. T.; Lynsky, C.; Godbe, J. M.; Sangji, H.; Luijten, E.; Stupp, S. I. Reversible self-assembly of superstructured networks. *Science* **2018**, *362*, 808−813.

(4) Van Hameren, R.; Schön, P.; Van Buul, A. M.; Hoogboom, J.; Lazarenko, S. V.; Gerritsen, J. W.; Engelkamp, H.; Christianen, P. C. M.; Heus, H. A.; Maan, J. C.; Rasing, T.; Speller, S.; Rowan, A. E.; Elemans, J. A. A. W.; Nolte, R. J. M. Macroscopic hierarchical surface patterning of porphyrin trimers via self-assembly and dewetting. *Science* **2006**, *314*, 1433−1436.

(5) Boekhoven, J.; Hendriksen, W. E.; Koper, G. J. M.; Eelkema, R.; Van Esch, J. H. Transient assembly of active materials fueled by a chemical reaction. *Science* **2015**, *349*, 1075−1079.

(6) Webber, M. J.; Appel, E. A.; Meijer, E. W.; Langer, R. Supramolecular biomaterials. *Nat. Mater.* **2016**, *15*, 13−26.

(7) Yan, X.; Liu, Z.; Zhang, Q.; Lopez, J.; Wang, H.; Wu, H. C.; Niu, S.; Yan, H.; Wang, S.; Lei, T.; Li, J.; Qi, D.; Huang, P.; Huang, J.; Zhang, Y.; Wang, Y.; Li, G.; Tok, J. B. H.; Chen, X.; Bao, Z. Quadruple H-bonding cross-linked supramolecular polymeric materials as substrates for stretchable, antitearing, and self-healable thin film electrodes. *J. Am. Chem. Soc.* **2018**, *140*, 5280−5289.

(8) Yamagishi, H.; Sato, H.; Hori, A.; Sato, Y.; Matsuda, R.; Kato, K.; Aida, T. Self-assembly of lattices with high structural complexity from a geometrically simple molecule. *Science* **2018**, *361*, 1242−1246.

(9) Reches, M.; Gazit, E. Casting metal nanowires within discrete self-assembled peptide nanotubes. *Science* **2003**, *300*, 625−627.

(10) Bera, S.; Mondal, S.; Xue, B.; Shimon, L. J. W.; Cao, Y.; Gazit, E. Rigid helical-like assemblies from a self-aggregating tripeptide. *Nat. Mater.* **2019**, *18*, 503−509.

(11) Chakraborty, P.; Guterman, T.; Adadi, N.; Yadid, M.; Brosh, T.; Adler-Abramovich, L.; Dvir, T.; Gazit, E. A Self-healing, all-organic, conducting, composite peptide hydrogel as pressure sensor and electrogenic cell soft substrate. *ACS Nano* **2019**, *13*, 163−175.

(12) Kumar, M.; Ing, N. L.; Narang, V.; Wijerathne, N. K.; Hochbaum, A. I.; Ulijn, R. V. Amino-acid-encoded biocatalytic self-assembly enables the formation of transient conducting nanostructures. *Nat. Chem.* **2018**, *10*, 696−703.

(13) Goujon, A.; Moulin, E.; Fuks, G.; Giuseppone, N. [c2]Daisy chain rotaxanes as molecular muscles. *CCS Chem.* **2019**, *1*, 83−96.

(14) Gu, Y.; Alt, E. A.; Wang, H.; Li, X.; Willard, A. P.; Johnson, J. A. Photoswitching topology in polymer networks with metal-organic cages as crosslinks. *Nature* **2018**, *560*, 65−69.

(15) Hendricks, M. P.; Sato, K.; Palmer, L. C.; Stupp, S. I. Supramolecular assembly of peptide amphiphiles. *Acc. Chem. Res.* **2017**, *50*, 2440−2448.

(16) Wang, Q.; Mynar, J. L.; Yoshida, M.; Lee, E.; Lee, M.; Okuro, K.; Kinbara, K.; Aida, T. High-water-content mouldable hydrogels by mixing clay and a dendritic molecular binder. *Nature* **2010**, *463*, 339−343.
(17) Sano, K.; Ishida, Y.; Aida, T. Synthesis of anisotropic hydrogels and their applications. *Angew. Chem., Int. Ed.* **2018**, *57*, 2532−2543.
(18) Sijbesma, R. P.; Beijer, F. H.; Brunsveld, L.; Folmer, B. J.; Hirschberg, J. K.; Lange, R. F.; Lowe, J. K. L.; Meijer, E. W. Reversible polymers formed from self-complementary monomers using quadruple hydrogen bonding. *Science* **1997**, *278*, 1601−1604.
(19) *Supramolecular Polymer Chemistry*; Harada, A., Ed.; Wiley-VCH: Weinheim, 2011.
(20) Doncom, K. E.; Blackman, L. D.; Wright, D. B.; Gibson, M. I.; O'Reilly, R. K. Dispersity effects in polymer self-assemblies: a matter of hierarchical control. *Chem. Soc. Rev.* **2017**, *46*, 4119−4134.
(21) Sun, C.; Shen, M.; Chavez, A. D.; Evans, A. M.; Liu, X.; Harutyunyan, B.; Flanders, N. C.; Hersam, M. C.; Bedzyk, M. J.; De La Cruz, M. O.; Dichtel, W. R. High aspect ratio nanotubes assembled from macrocyclic iminium salts. *Proc. Natl. Acad. Sci. U. S. A.* **2018**, *115*, 8883−8888.
(22) Wei, P.; Yan, X.; Huang, F. Supramolecular polymers constructed by orthogonal self-assembly based on host−guest and metal−ligand interactions. *Chem. Soc. Rev.* **2015**, *44*, 815−832.
(23) Lehn, J. M. Perspectives in chemistry—steps towards complex matter. *Angew. Chem., Int. Ed.* **2013**, *52*, 2836−2850.
(24) Aida, T.; Meijer, E. W.; Stupp, S. I. Functional supramolecular polymers. *Science* **2012**, *335*, 813−817.
(25) Vantomme, G.; Meijer, E. W. The construction of supramolecular systems. *Science* **2019**, *363*, 1396−1397.
(26) Rutten, M. G. T. A.; Vaandrager, F. W.; Elemans, J. A. A. W.; Nolte, R. J. M. Encoding information into polymers. *Nat. Rev. Chem.* **2018**, *2*, 365−381.
(27) Zhang, Q.; Shi, C. Y.; Qu, D. H.; Long, Y. T.; Feringa, B. L.; Tian, H. Exploring a naturally tailored small molecule for stretchable, self-healing, and adhesive supramolecular polymers. *Sci. Adv.* **2018**, *4*, No. eaat8192.
(28) Wang, S.; Xu, J.; Wang, W.; Wang, G.; Rastak, R.; Molina-Lopez, F.; Chung, J. W.; Niu, S.; Feig, V. R.; Lopez, J.; Lei, T.; Kwon, S. K.; Kim, Y.; Foudeh, A. M.; Ehrlich, A.; Gasperini, A.; Yun, Y.; Murmann, B.; Tok, J. B. H.; Bao, Z. Skin electronics from scalable fabrication of an intrinsically stretchable transistor array. *Nature* **2018**, *555*, 83−88.
(29) Kim, Y.; Chortos, A.; Xu, W.; Liu, Y.; Oh, J. Y.; Son, D.; Kang, J.; Foudeh, A. M.; Zhu, C.; Lee, Y.; Niu, S.; Liu, J.; Pfattner, R.; Bao, Z.; Lee, T. W. A bioinspired flexible organic artificial afferent nerve. *Science* **2018**, *360*, 998−1003.
(30) Son, D.; Kang, J.; Vardoulis, O.; Kim, Y.; Matsuhisa, N.; Oh, J. Y.; To, J. W. F.; Mun, J.; Katsumata, T.; Liu, Y.; McGuire, A. F.; Krason, M.; Molina-Lopez, F.; Ham, J.; Kraft, U.; Lee, Y.; Yun, Y.; Tok, J. B. H.; Bao, Z. An integrated self-healable electronic skin system fabricated via dynamic reconstruction of a nanostructured conducting network. *Nat. Nanotechnol.* **2018**, *13*, 1057−1065.
(31) Xu, J.; Wang, S.; Wang, G. J. N.; Zhu, C.; Luo, S.; Jin, L.; Rondeau-Gagné, S.; Park, S.; Schroeder, B. C.; Lu, C.; Lu, C.; Oh, J. Y.; Wang, Y.; Kim, Y. H.; Yan, H.; Sinclair, R.; Zhou, D.; Xue, G.; Murmann, B.; Linder, C.; Cai, W.; Tok, J. B. H.; Chung, J. W.; Bao, Z.; et al. Highly stretchable polymer semiconductor films through the nanoconfinement effect. *Science* **2017**, *355*, 59−64.
(32) Nan, K.; Kang, S. D.; Li, K.; Yu, K. J.; Zhu, F.; Wang, J.; Dunn, A. C.; Zhou, C.; Xie, Z.; Agne, M. T.; Wang, H.; Luan, H.; Zhang, Y.; Huang, Y.; Synder, G. J.; Rogers, J. A. Compliant and stretchable thermoelectric coils for energy harvesting in miniature flexible devices. *Sci. Adv.* **2018**, *4*, No. eaau5849.
(33) Miyajima, D.; Araoka, F.; Takezoe, H.; Kim, J.; Kato, K.; Takata, M.; Aida, T. Ferroelectric columnar liquid crystal featuring confined polar groups within core−shell architecture. *Science* **2012**, *336*, 209−213.
(34) Xia, Y.; Mathis, T. S.; Zhao, M. Q.; Anasori, B.; Dang, A.; Zhou, Z.; Cho, H.; Gogotsi, Y.; Yang, S. Thickness-independent capacitance of vertically aligned liquid-crystalline MXenes. *Nature* **2018**, *557*, 409−412.
(35) Nyström, G.; Arcari, M.; Mezzenga, R. Confinement-induced liquid crystalline transitions in amyloid fibril cholesteric tactoids. *Nat. Nanotechnol.* **2018**, *13*, 330−336.
(36) Arazoe, H.; Miyajima, D.; Akaike, K.; Araoka, F.; Sato, E.; Hikima, T.; Kawamoto, M.; Aida, T. An autonomous actuator driven by fluctuations in ambient humidity. *Nat. Mater.* **2016**, *15*, 1084−1089.
(37) Gelebart, A. H.; Mulder, D. J.; Varga, M.; Konya, A.; Vantomme, G.; Meijer, E. W.; Selinger, R. L. B.; Broer, D. J. Making waves in a photoactive polymer film. *Nature* **2017**, *546*, 632−636.
(38) Lv, J. A.; Liu, Y.; Wei, J.; Chen, E.; Qin, L.; Yu, Y. Photocontrol of fluid slugs in liquid crystal polymer microactuators. *Nature* **2016**, *537*, 179−184.
(39) Eelkema, R.; Pollard, M. M.; Vicario, J.; Katsonis, N.; Ramon, B. S.; Bastiaansen, C. W.; Broer, D. J.; Feringa, B. L. Nanomotor rotates microscale objects. *Nature* **2006**, *440*, 163.
(40) Ware, T. H.; McConney, M. E.; Wie, J. J.; Tondiglia, V. P.; White, T. J. Voxelated liquid crystal elastomers. *Science* **2015**, *347*, 982−984.
(41) Trigg, E. B.; Gaines, T. W.; Maréchal, M.; Moed, D. E.; Rannou, P.; Wagener, K. B.; Stevens, M. J.; Winey, K. I. Self-assembled highly ordered acid layers in precisely sulfonated polyethylene produce efficient proton transport. *Nat. Mater.* **2018**, *17*, 725−731.
(42) Song, J.; Chen, C.; Zhu, S.; Zhu, M.; Dai, J.; Ray, U.; Li, Y.; Kuang, Y.; Li, Y.; Quispe, N.; Yao, Y.; Gong, A.; Leiste, U. H.; Bruck, H. A.; Zhu, J. Y.; Vellore, A.; Li, H.; Minus, M. L.; Jia, Z.; Martini, A.; Li, T.; Hu, L. Processing bulk natural wood into a high-performance structural material. *Nature* **2018**, *554*, 224−228.
(43) Kristufek, S. L.; Wacker, K. T.; Tsao, Y.-Y.; Su, L.; Wooley, K. L. Monomer design strategies to create natural product-based polymer materials. *Nat. Prod. Rep.* **2017**, *34*, 433−459.
(44) Yu, Z.; Tantakitti, F.; Yu, T.; Palmer, L. C.; Schatz, G. C.; Stupp, S. I. Simultaneous covalent and noncovalent hybrid polymerizations. *Science* **2016**, *351*, 497−502.
(45) Barltrop, J. A.; Hayes, P. M.; Calvin, M. The chemistry of 1,2-dithiolane (trimethylene disulfide) as a model for the primary quantum conversion act in photosynthesis. *J. Am. Chem. Soc.* **1954**, *76*, 4348−4367.
(46) Fava, A.; Iliceto, A.; Camera, E. Kinetics of the thiol-disulfide exchange. *J. Am. Chem. Soc.* **1957**, *79*, 833−838.
(47) Zhang, X.; Waymouth, R. M. 1,2-Dithiolane-derived dynamic, covalent materials: cooperative self-assembly and reversible cross-linking. *J. Am. Chem. Soc.* **2017**, *139*, 3822−3833.
(48) Singh, G.; Chan, H.; Baskin, A.; Gelman, E.; Repnin, N.; Král, P.; Klajn, R. Self-assembly of magnetite nanocubes into helical superstructures. *Science* **2014**, *345*, 1149−1153.
(49) Dong, S.; Leng, J.; Feng, Y.; Liu, M.; Stackhouse, C. J.; Schönhals, A.; Chiappisi, L.; Gao, L.; Chen, W.; Shang, J.; Jin, L.; Qi, Z.; Schalley, C. A. Structural water as an essential comonomer in supramolecular polymerization. *Sci. Adv.* **2017**, *3*, No. eaao0900.
(50) Zhang, Q.; Li, T.; Duan, A.; Dong, S.; Zhao, W.; Stang, P. J. Formation of a supramolecular polymeric adhesive via water-participant hydrogen bond formation. *J. Am. Chem. Soc.* **2019**, *141*, 8058−8063.
(51) Van Zee, N. J.; Adelizzi, B.; Mabesoone, M. F.; Meng, X.; Aloi, A.; Zha, R. H.; Lutz, M.; Filot, I. A. W.; Palmans, A. R. A.; Meijer, E. W. Potential enthalpic energy of water in oils exploited to control supramolecular structure. *Nature* **2018**, *558*, 100−103.
(52) Yanagisawa, Y.; Nan, Y.; Okuro, K.; Aida, T. Mechanically robust, readily repairable polymers via tailored noncovalent cross-linking. *Science* **2018**, *359*, 72−76.
(53) De Haan, L. T.; Verjans, J. M.; Broer, D. J.; Bastiaansen, C. W.; Schenning, A. P. Humidity-responsive liquid crystalline polymer actuators with an asymmetry in the molecular trigger that bend, fold, and curl. *J. Am. Chem. Soc.* **2014**, *136*, 10585−10588.

DOI: 10.1021/jacs.9b05740
J. Am. Chem. Soc. 2019, 141, 12804−12814

(54) Ma, M.; Guo, L.; Anderson, D. G.; Langer, R. Bio-inspired polymer composite actuator and generator driven by water gradients. *Science* **2013**, *339*, 186−189.
(55) Lloyd, E. M.; Lopez Hernandez, H.; Feinberg, A. M.; Yourdkhani, M.; Zen, E. K.; Mejia, E. B.; Sottos, N. R.; Moore, J. S.; White, S. R. Fully recyclable metastable polymers and composites. *Chem. Mater.* **2019**, *31*, 398−406.
(56) Zou, Z.; Zhu, C.; Li, Y.; Lei, X.; Zhang, W.; Xiao, J. Rehealable, fully recyclable, and malleable electronic skin enabled by dynamic covalent thermoset nanocomposite. *Sci. Adv.* **2018**, *4*, No. eaaq0508.
(57) Christensen, P. R.; Scheuermann, A. M.; Loeffler, K. E.; Helms, B. A. Closed-loop recycling of plastics enabled by dynamic covalent diketoenamine bonds. *Nat. Chem.* **2019**, *11*, 442−448.
(58) Miller, K. A.; Morado, E. G.; Samanta, S. R.; Walker, B. A.; Nelson, A. Z.; Sen, S.; Tran, D. T.; Whitaker, D. J.; Ewoldt, R. H.; Braun, P. V.; Zimmerman, S. C. Acid-triggered, acid-generating, and self-amplifying degradable polymers. *J. Am. Chem. Soc.* **2019**, *141*, 2838−2842.
(59) Zhu, J. B.; Watson, E. M.; Tang, J.; Chen, E. Y. X. A synthetic polymer system with repeatable chemical recyclability. *Science* **2018**, *360*, 398−403.
(60) Rahimi, A.; García, J. M. Chemical recycling of waste plastics for new materials production. *Nat. Rev. Chem.* **2017**, *1*, 0046.

DOI: 10.1021/jacs.9b05740
J. Am. Chem. Soc. 2019, 141, 12804−12814